Obrabotka metallov (tekhnologiya, oborudovanie, instrumenty) = Metal Working and Material Science. 2024 vol. 26 no. 2 pp. 6–22
ISSN: 1994-6309 (print) / 2541-819X (online)
DOI: 10.17212/1994-6309-2024-26.2-6-22

NSTU NETI

Obrabotka metallov -
Metal Working and Material Science

Journal homepage: http://journals.nstu.ru/obrabotka_metallov

Investigations on ultrasonic vibration-assisted friction stir welded AA7075 joints: Mechanical properties and fracture analysis

Vaibhav Gaikwad [a, *], *Satish Chinchanikar* [b]

Vishwakarma Institute of Information Technology, Survey No. 3/4, Kondhwa (Budruk), Pune – 411048, Maharashtra, India

[a] https://orcid.org/0000-0002-3818-1893, vaibhav.219p0007@viit.ac.in; [b] https://orcid.org/0000-0002-4175-3098, satish.chinchanikar@viit.ac.in

ARTICLE INFO

Article history:
Received: 06 January 2024
Revised: 09 February 2024
Accepted: 20 March 2024
Available online: 15 June 2024

Keywords:
Friction stir welding
Shot peening
Fracture analysis
Ultrasonic vibrations
AA7075

ABSTRACT

Introduction. Joint efficiency and strength, particularly in aluminum alloys, are crucial in aerospace, defense, and industrial applications. Post-welding treatments like shot peening and laser shock peening significantly improve joint efficiency and strength, enhancing fatigue life, grain structure, and tensile strength. **The purpose of the work.** The literature reviewed shows that the ultrasonic vibration-assisted friction stir welding (*UVaFSW*) and post-weld treatment improved the mechanical properties and material flow. However, limited studies have been observed on the *UVaFSW* joints of *AA7075-T651*, considering the consequence of welding speed, tool rotation, and post-weld shot peeing treatment. **The methods of investigation.** The study investigates the ultrasonic vibration-assisted friction stir welded (*UVaFSWed*) *AA7075-T651* joint's tensile strength, microhardness, microstructure, and fracture behavior, considering the impact of tool rotation, welding speed, and post-weld shot peening treatment. **Results and Discussion.** The post-weld treated shot-peened *UVaFSWed* joints demonstrated the maximum tensile strength of 373.43 MPa, the microhardness of 161 HV, and the lowest surface roughness of 15.16 µm at 40 mm/min welding speed when compared to the friction stir-welded (*FSWed*) joints. These results indicate that shot peening improved the mechanical properties and surface quality of the *UVaFSWed* joints. The high tensile strength and low surface roughness make these joints suitable for applications requiring strength and aesthetics. The fracture for the shot peened *UVaFSWed* joints mainly occurred in the heat-affected zone (*HAZ*) during the tensile test. It could be attributed to the higher temperature experienced during welding, which resulted in grain growth and decreased material strength in the *HAZ*. The shot-peened *UVaFSWed* joint has a more uniform grain distribution than the *FSWed* one, which contributed to the joint's higher tensile strength. The fractured surface of the shot peened *UVaFSWed* joints showed larger, equiaxed, and shallow dimples, resulting in higher ultimate tensile strength (*UTS*) and microhardness compared to the conventional *FSWed* joints. The mechanical properties and microstructure observed in the welding zones of shot peened *UVaFSWed* joints are superior to those of conventional *FSW* joints. However, further investigation is required to determine the specific factors contributing to this localized failure at *HAZ*, considering the effects of shot peening parameters. This study also suggests the potential for optimizing shot peened *UVaFSWed* joints of *AA7075-T651*.

For citation: Gaikwad V., Chinchanikar S. Investigations on ultrasonic vibration-assisted friction stir welded AA7075 joints: Mechanical properties and fracture analysis. *Obrabotka metallov (tekhnologiya, oborudovanie, instrumenty) = Metal Working and Material Science*, 2024, vol. 26, no. 2, pp. 6–22. DOI: 10.17212/1994-6309-2024-26.2-6-22. (In Russian).

Introduction

Recently, there has been a trend in various industries to find innovative and cost-effective ways to reduce the weight of its products, increase the speed of its vehicles, airplanes and missiles, as well as reduce greenhouse gas emissions produced during manufacturing. Therefore, research continues on innovative joining techniques to realize material compounds and to get closer to the goals outlined above. *AA7075* aluminum alloy finds wide applications in the aerospace, defense, military, and automotive industries due to its low density and high mechanical properties. It is a precipitation hardening alloy with magnesium,

*** Corresponding author**
Gaikwad Vaibhav, Ph.D. (Engineering)
Vishwakarma Institute of Information Technology,
Survey No. 3/4, Kondhwa (Budruk),
Pune – 411048, Maharashtra, India
Tel.: 91-20269502401, **e-mail**: vaibhav.219p0007@viit.ac.in

zinc, and copper as the main alloying elements. Due to solidification and liquation cracking in the fusion welding, Friction stir welding (*FSW*) is preferred to joining aluminum alloys [1].

The *FSW* process is preferred for joining difficult-to-weld similar and dissimilar aluminum alloys. As a solid-state joining process, *FSW* tends to lower distortion and residual stress in the welded joints. In comparison to the fusion welding techniques, *FSW* provides better joints. A specially designed rotating tool is inserted into the edges of the workpiece to be joined and moved along the interface of two plates in the *FSW* process. Consequently, the softened material near the tool is transported from the advancing side to the retreating side to form a joint [2]. In the *FSW*, a high downward force and spindle torque are required to generate a large amount of heat. The heat generated softens the material, providing the adequate plastic flow next to the tool. This leads to an increase in the volume of welding equipment and a greater welding load [3].

The *FSW* tool pin profile is subjected to higher stress during welding, which causes rapid tool degradation, leading to premature failure. Moreover, tool wear causes poor weld quality, resulting in higher production costs. Also, the higher welding load in the *FSW* limits the welding speed. These difficulties can be solved using different secondary energy sources during *FSW*. A group of researchers applied ultrasonic vibrations during *FSW*. Ultrasonic vibration-assisted friction stir welding (*UVaFSW*) assists in softening of the material without substantial heating [4–6].

Liu et al. [7] found that ultrasonic vibration-assisted *FSW* improved the joint mechanical properties, the quality of the weld, and the heat input at the localized area. According to *Xu et al.* [8], brazing with ultrasonic vibration assistance created a junction with a smaller grain size that improved corrosion resistance and ultimate tensile strength (*UTS*). *Liu et al.* [9], while investigating *UVaFSW* of *AA1060* aluminum alloy, have found that ultrasonic energy enhanced the flow velocity, the volume of deformed material, and the strain rate.

In aerospace, defense sectors and industrial applications, joint efficiency, and joint strength, play a key role, especially for joints made of similar and dissimilar aluminum alloys. It has been widely reported that joint efficiency and strength can be substantially improved using post-welding treatment. In the last few years, researchers have focused on post-weld treatment for aluminum joints. Shot peening and laser shock peening treatments are prominently reported in the literature as post-weld treatment, since both processes induce residual compressive stresses in the welded specimen and improve fatigue life, grain structure, and tensile strength. Fig. 1, *a* and *b* shows the schematic diagrams of laser shock peening and shot peening, respectively.

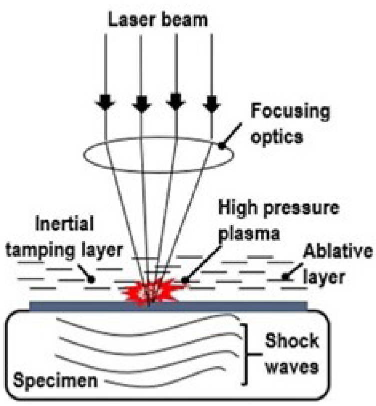

a

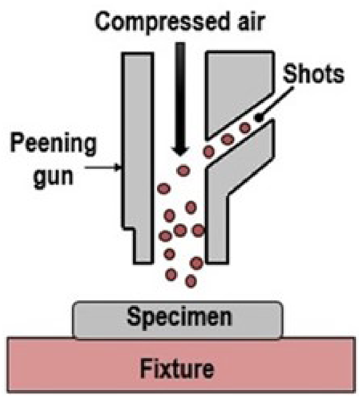

b

Fig. 1. Schematics of (*a*) Laser shock peening process, (*b*) Shot peening process

Amuda et al. in [10] inspected the effect of cryogenic cooling and the addition of element metal powder during the gas tungsten arc welding of the *AISI 430* plate. Their study showed that both strategies refined the grain structure. However, with the accumulation of metal powder, a significant decrease in the zone of thermal influence (*HAZ*) is found to be up to 50 %, and cryogenic cooling reduces *HAZ* to 36 %. On the other hand, cryogenic cooling led to an increase in the ductility of the joint by 80 % compared to the base metal (*BM*), whereas the addition of element metal powder led to an increase in the joint ductility by up to 60 %. *Hatamleh et al.* in [11] examined the effect of laser-peening, shot-peening, and cryogenic cooling on fatigue crack development and residual stresses of friction stir welded (*FSWed*) *AA2195* aluminum alloy joints. Their study found that fatigue crack development for the specimen treated with laser peening was the same as that of shot-peening and as-welding at ambient temperature. In addition, it was difficult to distinguish crack growth from residual stresses during cryogenic treatment.

Hatamleh et al. in [12] investigated the effect of laser shock peening and shot peening on the *FSWed* joint of the *AA2195* aluminum alloy. Their study observed improved mechanical properties with laser peening compared to shot peening. They observed an increase in the yield strength in the weld nugget (*WN*) by about 38 % when laser welding was used as post-welding treatment, compared with an increase in the yield strength in the weld nugget (*WN*) by 8 % observed during shot peening. *Khorrami et al.* in [13] investigated the effect of cryogenic and ambient temperature on the *FSW* of severely deformed *AA1050* aluminum alloy with *SiC* nanoparticles. Their work observed bimodal and finer grain sizes when using *FSW* joints with cryogenic cooling treatment as a measure against abnormal grain growth during the *FSW*.

Singh et al. in [14] performed the cryogenic treatment after the *FSW* on a joint of *AA7075* aluminum alloy. Their experimental study showed that post-weld cryogenic treatment led to a slight increase in the hardness of the joint and tensile strength. *Wang et al.* [15] inspected the effect of low-temperature aging and cryogenic treatment on the mechanical properties of the *FSWed AA2024-T351* aluminum alloy. The elimination of softened zones near the *HAZ* was noted due to a single low-temperature aging. However, due to a single low-temperature aging, a decrease in the strength of the joint was noted.

Wang et al. [16] performed the cryogenic treatment during *FSW* of the *Cu* joint. Their experimental work showed that grain refinement in the *WN* increased initially with increase in the rotational speed. However, it was observed to decrease with further increases in rotational speed. *Zhemchuzhnikova et al.* [17] observed extensive grain refinement and increase in the tensile strength of cryogenically treated *Al-Mg-Sc-Zr FSW* joints. *Ferreira et al.* [18] examined the effect of the glass and steel beads in shot peening on the welded joint. They noticed better results in fatigue and tensile strength with glass beads than with steel beads. Also, higher surface roughness was observed when using the steel beads as compared to glass beads.

A group of researchers [19–21] investigated the effect of laser shock peening on the microstructural properties, fatigue properties, and corrosion resistance of *FSWed* aluminum alloy joints. They observed a finer grain size, better corrosion resistance, and higher fatigue strength with laser shock peening-treated joints as compared to joints without laser shock peening as a post-welding treatment. However, more studies are required in post-weld treatments to obtain better mechanical properties for the welded joint.

The literature reviewed shows that the *UVaFSW* and post-weld treatment improved the mechanical properties and material flow. However, limited studies have been conducted on the *UVaFSW* joints of *AA7075-T651*, considering the consequence of welding speed, tool rotation, and post-weld shot peeing treatment. With this interpretation, the current work comparatively evaluates the performance of untreated and post-weld shot-peened ultrasonic vibration-assisted friction stir welded (*UVaFSWed*) *AA7075-T651* joints, taking into account the effect of welding speed and tool rotation. The performance is evaluated in terms of microhardness in the different regions of the weld, ultimate tensile strength (*UTS*), surface roughness, microstructure evaluation, and fracture analysis using scanning electron microscopy (*SEM*) images. The experiments were performed with conical threaded tool pin-type. The results are compared with the available literature on *FSW* of *AA7075*-T651 joints produced by means of conical threaded and conical tool pin profiles.

Experimental Design

In the present study, the square butt joint of *AA7075-T651* was produced using *UVaFSW*. The *UVaFSW* experimental setup is depicted in Fig. 2. Experiments were carried out with welding speeds of 20, 28, and 40 mm/min and tool rotations of 1,000; 1,400 and 2,000 rpm. The experiments were carried out using conical threaded tool on a universal milling machine. The two plates to be welded originally had a rectangular shape and were deburred.

The faying edges of the plates were machined into a smooth surface and cleaned with acetone. The ultrasonic vibrations generated by the ultrasonic transducer propagated through an amplitude transformer to expand the amplitude and focus the energy at the weld line of two plates. This energy was transmitted to the localized workpieces near and in advance of the *FSW* tool by a sonotrode. An output power of 1.2 kW and an ultrasonic vibration frequency of 20 kHz were used in the welding process. In the absence of a load, a vibration amplitude of 24 μm was used. The sonotrode was placed at an angle of 45° to the plane of the workpiece and at a distance of 20 mm from the *FSW* tool.

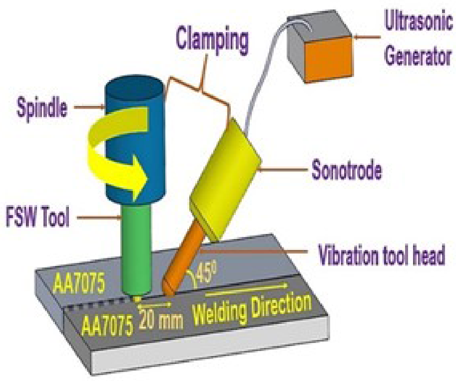

a

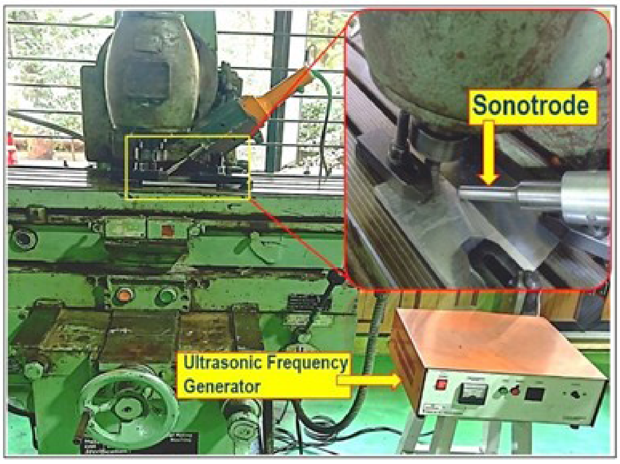

b

Fig. 2. Schematic view (*a*), Actual experimental setup (*b*)

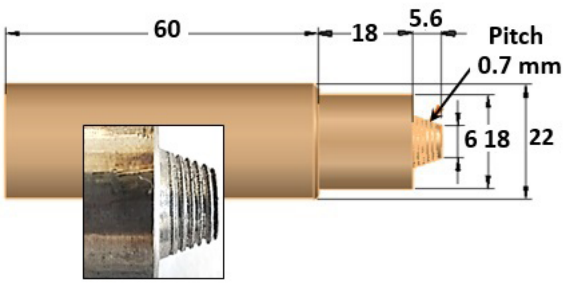

Fig. 3. Conical threaded pin type tool (All dimensions are in mm)

The tool with translational and rotational motions provides thermo-mechanical action along the welding path. The conical threaded tool pin profile with flat shoulder made of tool steel type *H13* is depicted in Fig. 3. The axial load on the work surface is transmitted by the tool shoulder. The plasticized material is transferred in to the weld pool by the pin. Tables 1 and 2 represent the chemical composition of the tool and the workpiece material respectively. In the present study, the shot peening process is selected as a post-weld treatment. The experimental set-up and parameters of the shot peening are depicted in Fig. 4.

The microstructure of the shot-peened *UVaFSWed* joints at different regions of the weld and the material flow in the *WN* were examined using *SEM* images. The mechanical properties of the joint, such as *UTS*, microhardness in *WN*, thermo-mechanically affected heat zone (*TMAZ*), *HAZ*, base metal, and surface roughness (*SR*), are inspected considering the influence of process variables.

The shot peened *UVaFSWed* joint transverse *UTS*, and joint efficiency were evaluated for all the joints obtained at different process parameters. The tensile test was performed on a universal testing machine according to the *ASTM E8* standard. Fig. 5, *a*, *b* shows a diagram of cutting a plate made of aluminum alloy *AA7075-T651* to obtain a test specimen and a tensile test specimen, respectively. The microhardness at *WN*, *TMAZ*, *HAZ*, and *BM* was measured using *Vicker's* microhardness tester in accordance with *ISO6507* standard by the means of diamond indenter (136°) through a load of 100 grams and an indentation time of 20 seconds. An average *SR*, measured at the start, middle, and end of the weld, was obtained.

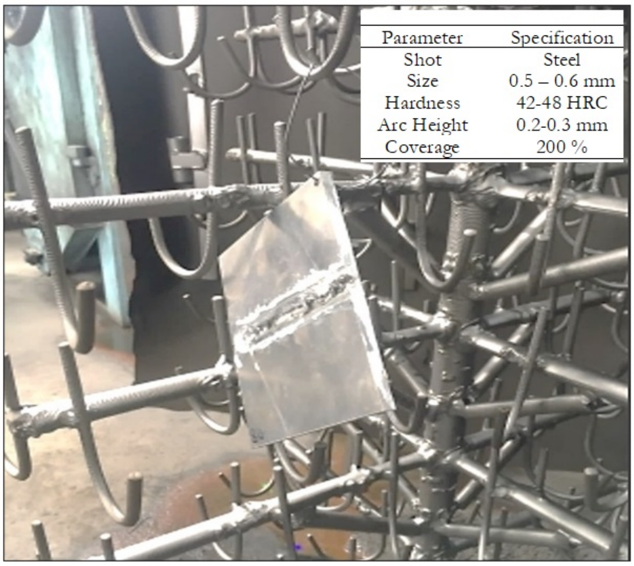

Fig. 4. Mounted specimen for shot peening

Table 1

Chemical composition of *H13 FSW* tool (% weight)

Elements	*Cr*	*Mo*	*Si*	*V*	*C*	*Ni*	*Cu*	*Mn*	*P*	*S*
% weight	4.75	1.10	0.80	0.80	0.32	0.3	0.25	0.2	0.03	0.03

Table 2

Chemical composition of *AA7075* alloy (% weight)

Elements	% weight	Elements	% weight	Elements	% weight	Elements	% weight
Si	0.069	*Mn*	0.006	*Ni*	0.012	*Ti*	0.028
Fe	0.204	*Mg*	2.33	*Pb*	0.012	*Cr*	0.195
Cu	1.64	*Zn*	5.28	*Sn*	< 0.005	*Al*	90.22

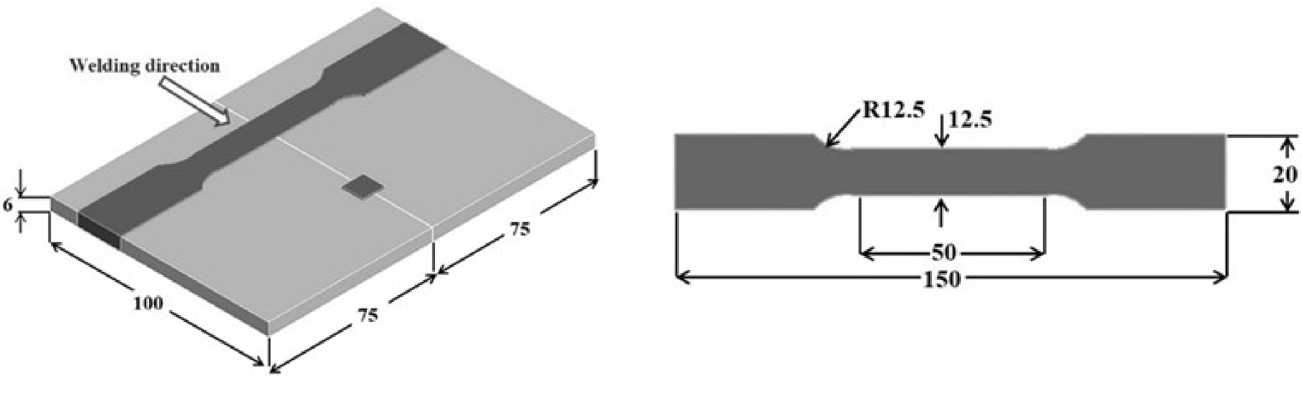

Fig. 5. AA7075 plates showing abstraction of test specimens (*a*), Tensile test specimen (*b*) (All dimensions are in mm)

A Field Emission Scanning Electron Microscope (*FESEM*) was used at several magnifications to examine the material flow in the *WN* and the joint microstructure at various welding zones. The specimens were cut in the perpendicular direction to the weld contour by wire electric discharge machining.

Results and Discussion

This section discusses the performance of shot-peened *UVaFSWed AA7075-T651* joints. Tensile strength, microhardness, fracture behavior, and microstructure of welded joints are assessed considering the effect of welding speed and tool rotation. The *UTS* of the *BM* attained after the tensile test is 550 MPa. For the shot-peened *UVaFSWed* (Run ***P1*** to ***P9***) the experimental matrix and mechanical properties are presented in Table 3.

Table 3

Experimental matrix with mechanical properties for shot-peened *UVaFSWed AA7075* joints

Run	Tool rotation (rpm)	Welding speed (mm/min)	UTS (MPa)	Joint efficiency (%)	Microhardness (HV)			Surface roughness (µm)
					WN	*TMAZ*	*HAZ*	
P1	1,000	20	301.98	54.91	148	129	119	15.350
P2	1,000	28	294.57	53.56	152	133	125	15.480
P3	1,000	40	292.32	53.15	154	143	130	16.341
P4	1,400	20	281.88	51.25	150	138	127	15.976
P5	1,400	28	304.20	55.31	158	145	129	18.277
P6	1,400	40	312.95	56.90	149	141	132	15.918
P7	2,000	20	345.73	62.86	155	145	135	17.672
P8	2,000	28	362.95	65.99	160	144	132	15.169
P9	2,000	40	373.43	67.90	161	145	136	15.651

Mechanical properties of shot peened UVaFSWed joints

Stress-strain curves for *AA7075-T651* shot-peened *UVaFSWed* joints (Run ***P1*** to ***P9***) are obtained. For the shot-peened *UVaFSWed AA7075-T651* aluminum alloy joints, the maximum *UTS* of 373.43 MPa (run P9) is obtained at tool rotation of 2,000 rpm and welding speed of 40 mm/min, whereas the minimum *UTS* of 281.88 MPa (Run ***P4***) is obtained at tool rotation of 1,400 rpm and welding speed of 20 mm/min. The *UTS* for the shot-peened *UVaFSWed AA7075* joints is compared to that obtained using traditional *FSW* with conical and conical threaded tool pin profiles [22–25]. This study found higher *UTS* for joints obtained using *UVaFSW*, followed by the shot-peening process.

In the shot peening, steel balls acted at high velocity on the *UVaFSWed* joint. This high velocity induces compressive residual stresses on the fabricated joint. This effect improves the *UTS* as well as the microhardness of the joint. Better performance, almost more than two times higher values of tensile strength, and joint efficiency can be seen for the shot-peened *UVaFSWed* joints compared to the *FSWed* joints with conical threaded tool pins [22–25]. The higher mechanical properties of the shot-peened *UVaFSWed* joints could be attributed to an increased strain rate leading to higher plastic deformation and better material flow around the tool pin due to the ultrasonic vibrations. A group of researchers observed better mechanical properties of the *UVaFSWed* joints made of similar-dissimilar aluminum alloy joints [7–9].

Higher values of *UTS* are obtained at a higher tool rotation speed. The higher the tool rotation speed, the greater the frictional heat between the tool shoulder and the surface of the workpiece. The increased frictional heat softens the material and enhances its movement to the weld pool, resulting in uniform mixing of the material. The microhardness of joints was measured at several points from the weld center on both sides of the joint. The dynamic recrystallization of grains and higher plastic deformation causes variations in the microhardness in the welded region. The microhardness of the shot peened *UVaFSWed* joints showed variation in the welding zones, mostly following the distribution of a letter '***W***'-shape, and found maximum at the *WN* and minimum at the *HAZ*. A higher microhardness was obtained in all the zones of the weld: *WN*, *TMAZ*, and *HAZ* for the shot peened *UVaFSWed* joints (Run ***P1-P9***) as compared to that obtained using traditional *FSW* with conical and conical threaded tool pin profiles [22–25]. This study found higher microhardness for joints obtained using *UVaFSW*, followed by the shot-peening process.

A higher microhardness in *WN* is obtained for shot-peened *UVaFSWed* joints at higher tool rotation speeds. The shot peening process imparts compressive residual stress on the fabricated joints, resulting in higher microhardness in the *WN*. The maximum microhardness in *WN* was 161 HV and was obtained at the higher tool rotation of 2,000 rpm for the shot-peened *UVaFSWed* (Runs ***P7-P9***) *AA7075-T651* aluminum alloy joints.

The shot-peened *UVaFSWed* joints showed better mechanical properties compared to *FSWed* joints. The shot-peened *UVaFSWed* joints sustained higher tensile loads, as shot-peening induces compressive stresses in the workpiece. *UVaFSWed* joints sustained higher tensile loads, which could be attributed to higher heat input due to the application of ultrasonic vibrations on the weld bead. Moreover, ultrasonic vibrations acting on the weld bead contributed to dynamic recrystallization and improved the material movement towards the weld bead. Further, the assistance of ultrasonic vibrations also reduced weld defects/flaws in the *WN* and its interfaces with *TMAZ* compared with the conventional *FSWed* joints. The joint quality was assessed by obtaining the surface roughness. An average surface roughness was 15–18 μm for shot-peened *UVaFSWed AA7075-T651* aluminum alloy joints. Lower surface roughness values were obtained at a lower tool rotation speed of 1,000 rpm, regardless of the welding speed (Runs ***P1-P3***).

Fig. 6 represents the top surface appearance of the shot-peened *UVaFSWed AA7075-T651* aluminum alloy joints. The surface modifications and filling of the weld bead can be seen. The "onion rings" are formed, and the tool shoulder marks can be seen.

Microstructure of shot-peened UVaFSWed joints

Fig. 7, *a*, c shows *SEM* images of *WN*, *TMAZ*, and *HAZ* of the shot-peened *UVaFSWed* joints obtained at Run ***P9***, respectively. The homogeneous grain distribution in *WN* and the absence of tunnel defects can be

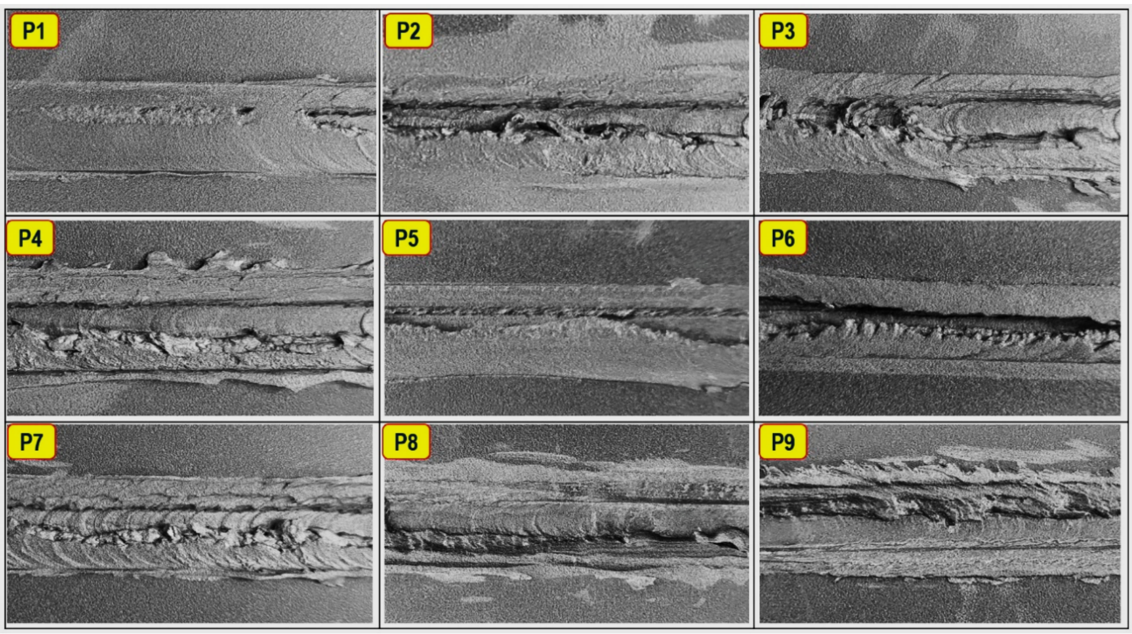

Fig. 6. Weld top surface of *AA7075 UVaFSWed* shot-peened joints

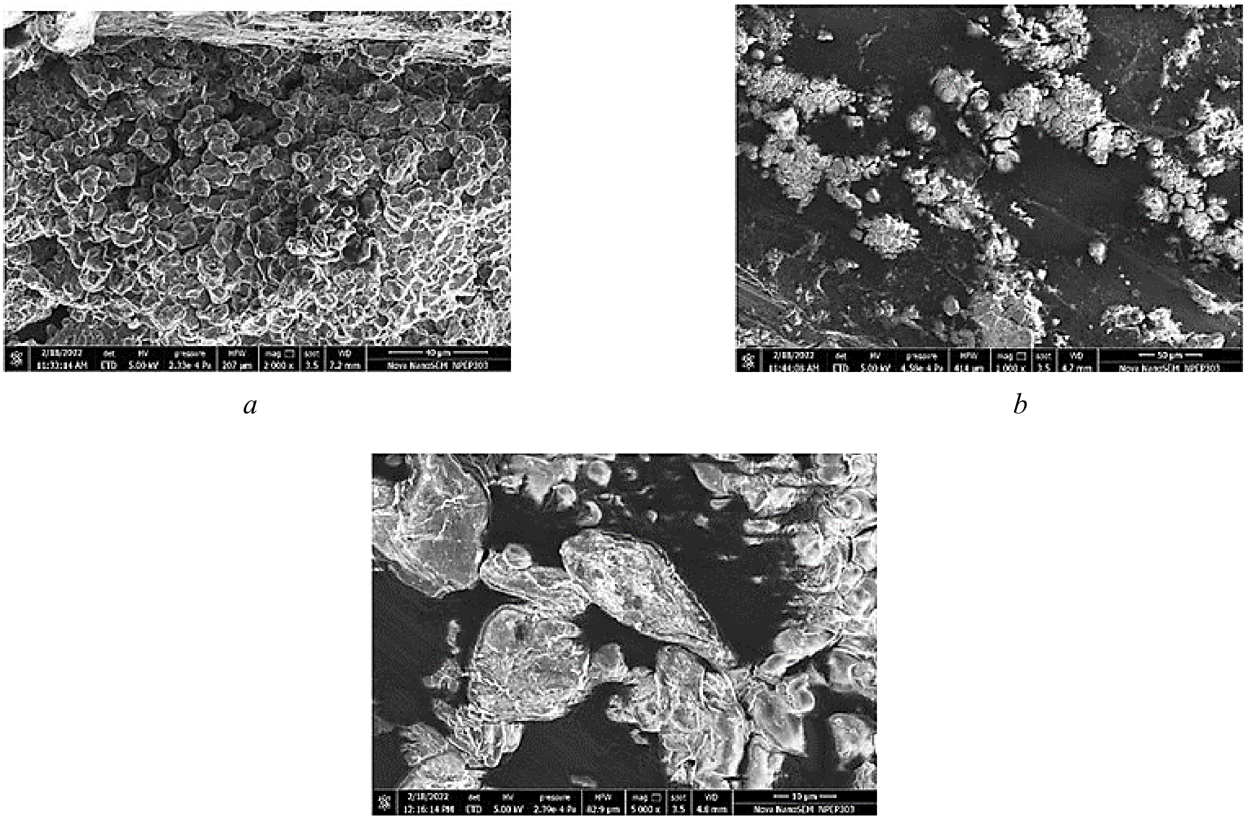

a *b* *c*

Fig. 7. SEM images of the shot-peened *UVaFSWed* joints at *WN* (*a*), *TMAZ* (*b*), and *HAZ* (*c*)

seen in Fig. 7, *a*. These attributes resulted in a higher *UTS* for the shot-peened *UVaFSWed* joint compared to the conventional *FSWed* joint. Fine, equiaxed, and uniformly distributed grains of ~630 nm-5 µm in the *WN* of the shot-peened *UVaFSWed* joint can be seen in Fig. 7, *a*. *UVaFSW* improves the grain size in *WN*, and the material flows inside the weld bead compared to the conventional *FSW*.

Fig. 7, *b* depicts the *SEM* image of *TMAZ* of the shot-peened *UVaFSWed* joint. Homogeneous mixing of the material with equiaxed grains can be seen. The coarser distributed grains than those in the *WN* differentiate this weld region. This weld region is adjacent to the *WN*. The grains having coarser sizes of ~ 5–7 µm can be seen in *TMAZ*. This could be due to lower heat distribution from the *WN* to *TMAZ*. Fig. 7, *c* depicts a *SEM* image of *HAZ* of a shot-peened *UVaFSWed* joint. Elongated grains with sizes varying in the range of ~8–11 µm can be seen. This weld zone is between *TMAZ* and *BM* and is designated as *HAZ*. The reduction in microhardness with an increase in grain size can be seen from the *WN* to *HAZ*. The highest microhardness observed in the *WN* was 161 HV, followed by 145 HV in *TMAZ* and 136 HV in *HAZ*.

SEM images show that shot-peened *UVaFSW* improves the grain size in the *WN* and the material flow inside the weld bead compared to the conventional *FSW* [21–25]. Fine, equiaxed, and uniformly distributed grains at the *WN* can be seen for the shot-peened *UVaFSWed* joint. The higher mechanical properties obtained for the shot-peened *UVaFSWed* joints can be confirmed from *SEM* images showing higher plastic deformation, dynamic recrystallization, and better material flow toward the weld bead.

Fracture behavior of UVaFSWed AA7075-T651 joints

Fig. 8 depicts the fractured specimens of shot-peened *UVaFSWed* joints of *AA7075-T651* that were obtained during Runs ***P1–P9***. These specimens were subjected to a tensile test, and the results were compared side by side. The study found that all the test specimens had fractured in the *HAZ* and exhibited ductile behavior during the fracture. Fig. 9 shows *SEM* images of a fracture surface of specimen of the shot-

Fig. 8. Fracture behavior of the shot-peened *UVaFSWed AA7075* joints

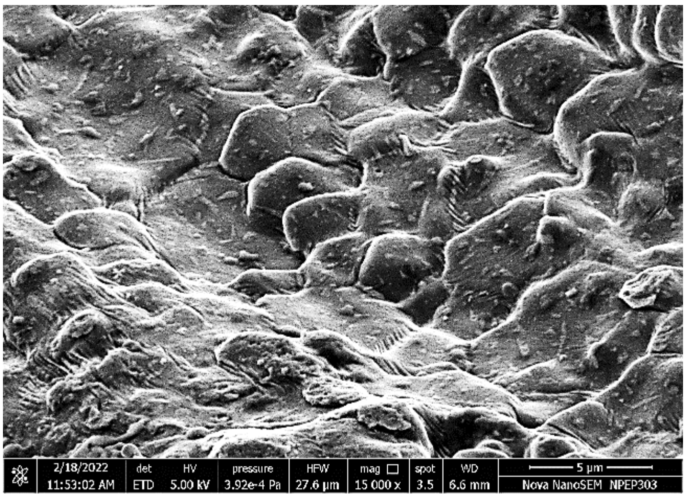

Fig. 9. SEM images of the fracture surface of shot-peened *UVaFSWed* joint of *AA7075*

peened *UVaFSWed* joint that was obtained during Run ***P9***. The large and shallow dimples in the shot-peened *UVaFSWed* test specimen show higher plastic deformation. The dimple sizes impact the sustainability of plastic deformation during tensile testing. The dimples observed on the shot-peened *UVaFSWed* specimen are larger and more equiaxed than that of the fractured conventional *FSWed* test specimen [22–25]. Hence, the *UTS* and microhardness in different weld regions are superior for shot-peened *UVaFSWed* joints compared to the conventional *FSWed* joint.

Researchers have observed different fracture patterns in shot-peened *UVaFSWed* joints. The reason for this is due to the heat generated during the process. The dual effect of ultrasonic vibration and frictional heat produced by the tool shoulder results in the release of more heat during *UVaFSW*. The higher the heat generation, the higher the plastic deformation and material flow, which ultimately results in higher values of *UTS* and microhardness. Additionally, a group of researchers have observed a correlation between the large and equiaxed dimples observed on the fracture surface with the higher values of *UTS* and microhardness of *FSWed* joints [26–28].

Material flow of the shot-peened UVaFSWed AA7075-T651 joints

During Friction Stir Welding (*FSW*), the quality of the weld depends on the flow of pasty material beneath the tool. Fig. 10 illustrates the material flow at the Weld Nugget (*WN*) for the shot-peened *UVaFSWed* joint *of AA7075-T651* at Run ***P9***. At Run ***P9***, the laminar material flow was observed. The microstructure of the shot-peened *UVaFSWed AA7075-T651* joints obtained at Run ***P9*** is free of defects and porosity compared to conventional *FSW* joints [22–25]. Fig. 10 shows that the material flow is unidirectional, indicating proper intermixing of the material in the *WN*. The proper intermixing of the material improves the mechanical properties of the joints. Due to the ultrasonic vibrations, tunnel defects and micro-voids are eliminated, and fusion between the materials is improved. This results in higher mechanical properties compared to conventional *FSWed* joints.

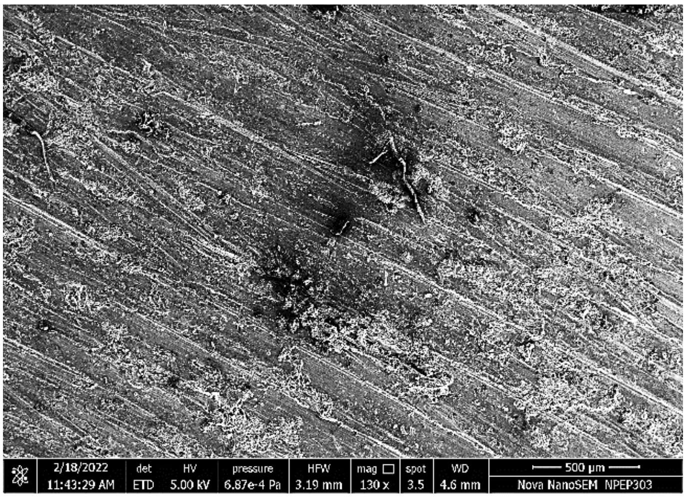

Fig. 10. Material flow of the shot-peened *UVaFSWed AA7075* joint

In the current study, it was observed that shot-peened *UVaFSWed AA7075-T651* joints exhibit superior mechanical properties, favorable microstructure, and ductile-type fracture behavior as compared to conventional *FSWed* joints. However, the shot peening and *UVaFSW* combination yielded even better results. Additional research is necessary to optimize shot-peened *UVaFSW* while considering various interlayers, process parameters, and tool-pin geometries.

Conclusions

This study aimed to evaluate the performance of *AA7075-T651* joints produced through shot-peened ultrasonic vibration-assisted friction stir welding (*UVaFSWed*) with a conical threaded pin type tool. The study varied the tool rotation and welding speeds to assess its impact on the joints tensile strength, micro-hardness, microstructure, and fracture behavior. Additionally, the study examined the grain distribution, material flow at the weld nugget, and joint fracture surfaces after the tensile test using *SEM* images. From the investigation, the following conclusions were made:

- The joint made by *UVaFSW* had better tensile strength, microhardness in the *WN*, and minimum surface roughness in comparison to traditionally *FSWed* joints. The shot-peened *UVaFSWed* joint is characterized by a maximum value of *UTS* (373.43 MPa) and microhardness in the *WN (*161 HV) at a tool rotation of

2,000 rpm and welding speed of 40 mm/min. However, it should be noted that when the welding speed was reduced to 28 mm/min, a lower surface roughness of 15.16 µm was obtained.

● The microhardness of the joints that underwent shot peening during the *UVaFSW* welding process showed variation in the welding zones, forming a letter '***W***' shape. The maximum microhardness value was observed in the *WN* zone while the minimum was found in *HAZ*. Additionally, the microhardness values were higher in shot-peened *UVaFSW* joints compared to conventional *FSWed* joints.

● Inspection of the shot-peened *UVaFSWed* joint has shown that the material fusion in the weld nugget was appropriate, there was a flow of pasty material, the joint was free of tunnel defects and voids, and there was a homogeneous distribution of finer grains. This was found to be superior to the conventional *FSWed* joints.

● All the test specimens for the shot-peened *UVaFSWed* joints were fractured in the *HAZ* due to lower microhardness, and it exhibited ductile behavior during fracture. The fractured surface of the shot-peened *UVaFSWed* joints showed larger, more equiaxed, and shallow dimples, resulting in higher ultimate tensile strength (*UTS*) and microhardness compared to the conventional *FSWed* joints.

● The mechanical properties and microstructure observed in the welding zones of shot-peened *UVaFSWed* joints are superior to those of conventional *FSW* joints. This study suggests the potential for optimizing the shot-peened *UVaFSWed* joints of *AA7075-T651*.

References

1. Cetkin E., Çelik Y.H., Temiz S. Microstructure and mechanical properties of AA7075/AA5182 jointed by FSW. *Journal of Materials Processing Technology*, 2019, vol. 268, pp. 107–116. DOI: 10.1016/j.jmatprotec.2019.01.005.

2. Chinchanikar S., Gaikwad V.S. State of the art in friction stir welding and ultrasonic vibration-assisted friction stir welding of similar/dissimilar aluminum alloys. *Journal of Computational and Applied Research in Mechanical Engineering*, 2021, vol. 11, pp. 67–100. DOI: 10.22061/JCARME.2021.7390.1983.

3. Arora A., De A., Debroy T. Toward optimum friction stir welding tool shoulder diameter. *Scripta Materialia*, 2011, vol. 64, pp. 9–12. DOI: 10.1016/j.scriptamat.2010.08.052.

4. Shi L., Wu C.S., Liu X.C. Modeling the effects of ultrasonic vibration on friction stir welding. *Journal of Materials Processing Technology*, 2015, vol. 222, pp. 91–102. DOI: 10.1016/j.jmatprotec.2015.03.002.

5. Yao Z., Kim G.Y., Faidley L., Zou Q., Mei D., Chen Z. Effects of superimposed high-frequency vibration on deformation of aluminum in micro/meso-scale upsetting. *Journal of Materials Processing Technology*, 2012, vol. 212, pp. 640–646. DOI: 10.1016/j.jmatprotec.2011.10.017.

6. Siddiq A., El Sayed T. Acoustic softening in metals during ultrasonic assisted deformation via CP-FEM. *Materials Letters*, 2011, vol. 65, pp. 356–359. DOI: 10.1016/j.matlet.2010.10.031.

7. Liu X.C., Wu C.S. Experimental study on ultrasonic vibration enhanced friction stir welding. *Proceedings of the 1st International Joint Symposium on Joining and Welding*, Osaka, Japan, 2013, pp. 151–154. DOI: 10.1533/978-1-78242-164-1.151.

8. Xu C., Sheng G., Cao X., Yuan X. Evolution of microstructure, mechanical properties and corrosion resistance of ultrasonic assisted welded-brazed Mg/Ti joint. *Journal of Materials Science and Technology*, 2016, vol. 32, pp. 1253–1259. DOI: 10.1016/j.jmst.2016.08.029.

9. Liu X., Wu C., Padhy G.K. Characterization of plastic deformation and material flow in ultrasonic vibration enhanced friction stir welding. *Scripta Materialia*, 2015, vol. 102, pp. 95–98. DOI: 10.1016/j.scriptamat.2015.02.022.

10. Amuda M.O.H., Mridha S. Comparative evaluation of grain refinement in AISI 430 FSS welds by elemental metal powder addition and cryogenic cooling. *Materials and Design*, 2012, vol. 35, pp. 609–618. DOI: 10.1016/j.matdes.2011.09.066.

11. Hatamleh O., Hill M., Forth S., Garcia D. Fatigue crack growth performance of peened friction stir welded 2195 aluminum alloy joints at elevated and cryogenic temperatures. *Materials Science and Engineering A*, 2009, vol. 519, pp. 61–69. DOI: 10.1016/j.msea.2009.04.049.

12. Hatamleh O., Mishra R.S., Oliveras O. Peening effects on mechanical properties in friction stir welded AA 2195 at elevated and cryogenic temperatures. *Materials and Design*, 2009, vol. 30, pp. 3165–3173. DOI: 10.1016/j.matdes.2008.11.010.

13. Khorrami M.S., Kazeminezhad M., Miyashita Y., Saito N., Kokabi A.H. Influence of ambient and cryogenic temperature on friction stir processing of severely deformed aluminum with SiC nanoparticles. *Journal of Alloys and Compounds*, 2017, vol. 718, pp. 361–372. DOI: 10.1016/j.jallcom.2017.05.234.

14. Singh S., Dhuria G. Investigation of post weld cryogenic treatment on weld strength in friction stir welded dissimilar aluminum alloys AA2014-T651 and AA7075-T651. *Materials Today Proceedings*, 2017, vol. 4, pp. 8866–8873. DOI: 10.1016/j.matpr.2017.07.237.

15. Wang J., Fu R., Li Y. Effects of deep cryogenic treatment and low-temperature aging on the mechanical properties of friction-stir-welded joints of 2024-T351 aluminum alloy. *Materials Science and Engineering A*, 2014, vol. 609, pp. 147–153. DOI: 10.1016/j.msea.2014.04.077.

16. Wang Y., Fu R., Jing L., Li Y., Sang D. Grain refinement and nanostructure formation in pure copper during cryogenic friction stir processing. *Materials Science and Engineering A*, 2017, vol. 703, pp. 470–476. DOI: 10.1016/j.msea.2017.07.090.

17. Zhemchuzhnikova D., Malopheyev S., Mironov S., Kaibyshev R. Cryogenic properties of Al-Mg-Sc-Zr friction-stir welds. *Materials Science and Engineering A*, 2014, vol. 598, pp. 387–395. DOI: 10.1016/j.msea.2014.01.060.

18. Ferreira N., Jesus J.S., Ferreira J.A.M., Capela C., Costa J.M., Batista A.C. Effect of bead characteristics on the fatigue life of shot peened Al 7475-T7351 specimens. *International Journal of Fatigue*, 2020, vol. 134, p. 105521. DOI: 10.1016/j.ijfatigue.2020.105521.

19. Liu P., Sun S., Hu J. Effect of laser shock peening on the microstructure and corrosion resistance in the surface of weld nugget zone and heat-affected zone of FSW joints of 7050 Al alloy. *Optics & Laser Technology*, 2019, vol. 112, pp. 1–7. DOI: 10.1016/j.optlastec.2018.10.054.

20. Sano Y., Masaki K., Gushi T., Sano T. Improvement in fatigue performance of friction stir welded A6061-T6 aluminum alloy by laser peening without coating. *Materials and Design*, 2012, vol. 36, pp. 809–814. DOI: 10.1016/j.matdes.2011.10.053.

21. Gaikwad V.S., Chinchanikar S. Mechanical behaviour of friction stir welded AA7075-T651 joints considering the effect of tool geometry and process parameters. *Advances in Materials and Processing Technologies*, 2022, vol. 8 (4), pp. 3730–3748. DOI: 10.1080/2374068X.2021.1976554.

22. Gaikwad V., Chinchanikar S., Manav O. Investigation and multi-objective optimization of friction stir welding of AA7075-T651 plates. *Welding International*, 2023, vol. 37 (2), pp. 68–78. DOI: 10.1080/09507116.2023.2177568.

23. Gaikwad V.S., Chinchanikar S.S. Adaptive neuro fuzzy inference system to predict the mechanical properties of friction stir welded AA7075-T651 joints. *Jordan Journal of Mechanical and Industrial Engineering*, 2022, vol. 16 (3), pp. 381–393.

24. Gaikwad V.S., Chinchanikar S. Mechanical properties, microstructure, and fracture behavior of friction stir welded AA7075 joints with conical pin and conical threaded pin type tools. *Scientia Iranica*, 2022, vol. 30, pp. 1–20. DOI: 10.24200/sci.2022.59154.6087.

25. Gaikwad V.S., Chinchanikar S. Investigation on surface roughness, ultimate tensile strength, and microhardness of friction stir welded AA7075-T651 joint. *Materials Today Proceedings*, 2021, vol. 46, pp. 8061–8065. DOI: 10.1016/j.matpr.2021.03.034.

26. Liu Z., Meng X., Ji S., Li Z., Wang L. Improving tensile properties of Al/Mg joint by smashing intermetallic compounds via ultrasonic-assisted stationary shoulder friction stir welding. *Journal of Manufacturing Processes*, 2018, vol. 31, pp. 552–559. DOI: 10.1016/j.jmapro.2017.12.022.

27. Gao S., Wu C.S., Padhy G.K. Material flow, microstructure and mechanical properties of friction stir welded AA 2024-T3 enhanced by ultrasonic vibrations. *Journal of Manufacturing Processes*, 2017, vol. 30, pp. 385–395. DOI: 10.1016/j.jmapro.2017.10.008.

28. Ji S., Meng X., Liu Z., Huang R., Li Z. Dissimilar friction stir welding of 6061 aluminum alloy and AZ31 magnesium alloy assisted with ultrasonic. *Materials Letters*, 2017, vol. 201, pp. 173–176. DOI: 10.1016/j.matlet.2017.05.011.

Conflicts of Interest

The authors declare no conflict of interest.